Electronic Supplementary Material (ESI) for Chemical Science.

Glucose/O_2 Fuel Cell-Based Self-Powered Biosensor for Probing Drug Delivery Model with Self-Diagnosis and Self-Evaluation

Linlin Wang,[a] Haohua Shao,[a] Xuanzhao Lu,[a] Wenjing Wang,[a] Jian-Rong Zhang,[a,b*] Rong-Bin Song,[a*] Jun-Jie Zhu[a*]

[a]State Key Laboratory of Analytical Chemistry for Life and Collaborative Innovation Center of Chemistry for Life Sciences, School of Chemistry and Chemical Engineering, Nanjing University, Nanjing 210093, P. R. China.

[b] School of Chemistry and Life Science, Nanjing University Jinling College, Nanjing 210089, P. R. China.

*Corresponding Authors: jrzhang@nju.edu.cn (J.-R. Z.); rbsong@nju.edu.cn (R.-B. S.); jjzhu@nju.edu.cn (J.-J. Z.).

CHEMICALS

Silver nitrate (≥ 99 %), hydroquinone (≥ 99 %), gold (III) chloride trihydrate (≥ 99.9 %), 1-ethyl-3-(3-dimethylaminopropyl) carbodiimide hydrochloride (EDC), N-hydroxysuccinimide (NHS), Doxorubicin hydrochloride (Dox), N-cetyltrimethylammonium bromide (CTAB), tetraethyl orthosilicate (TEOS), sodium hydroxide, (3-aminopropyl)triethoxysilane (APTES, 99%), (2-(Acryloyloxy)ethyl) trimethylammoniumchloride (AETAC, 80 wt% in water) and 2,2-azobis(2-methylpropionamidine) dihydrochloride (V-50, >97.0%) were purchased from Sigma-Aldrich (St. Louis, USA). 3-(4,5-Dimethylthiazol-2-yl)-2,5-diphenyltetrazolium bromide (MTT) was obtained from Sunshine Biotech. Co. Ltd. (Nanjing, China). Phosphate buffer saline (PBS, 10 mM, pH = 7.4) contained 136.7 mM NaCl, 2.7 mM KCl, 8.7 mM Na_2HPO_4 and 1.4 mM KH_2PO_4, ethylene glycol, ammonia solution and dimethyl sulfoxide (DMSO) were purchased from Nanjing Chemical Reagent Co., Ltd. Hydrochloric acid (37%), poly(vinyl pyrrolidone) (PVP K-30) were purchased from Sinopharm Chemical Reagent Co., Ltd. Sodium hyaluronate (Mw ~100,000) and hyaluronidase (HAase) were purchased from Aladdin. All other reagents were of analytical grade and used without purification. The oligonucleotides and phosphatidylserine (PS)-binding peptide used in this paper were purchased from Shanghai Sangon Biological Engineering Technology & Services Co. (China). The sequences are as follows:

PSD: 5’-SH-C6-GGCTCCCAAGAACCTCACCTGTTGGAGTGGACA-C6-NH_2-3’

miR-125a: 5’-ACAGGUGAGGUUCUUGGGAGCC-3’

miR-21: 5’-UAGCUUAUCAGACUGAUGUUGA-3’

INSTRUMENTS

UV-vis spectra were recorded on a UV-3600 spectrophotometer (Shimadzu, Kyoto, Japan). Transmission electron micrographs (TEM) were measured on a JEOL JEM 200CX transmission electron microscope, using an accelerating voltage of 200 kV. The ordered structures of the pAuNB materials were confirmed by XRD on a Thermo ARL SCINTAG X’TRA diffractometer using a Cu-Kα radiation (λ =0.15405 nm). N_2 adsorption-desorption isotherms were recorded on a Micromeritics ASAP 2020M automated sorption analyzer. The samples were degassed at 300 ºC for 3 h. The specific surface areas were calculated from the adsorption data in low pressure range using the Brunauer-Emmett-Teller (BET) modal, and pore size was determined following the Barret-Joyner-Halenda (BJH) method. Confocal laser scanning microscopy (CLSM) studies were performed using a Leica TCS SP5 microscope (Germany) with excitation at 405 nm. Flow cytometric analysis was recorded using Cytomics FC 500 MCL (BECKMAN COULTER, U.S.A.).

MTT assays were recorded at 490 nm using a Bio-Rad 680 microplate reader. Electrochemical experiments were performed with a CHI 660C workstation (Shanghai Chenhua Apparatus Corporation, China). Polarization curves of the sensor were measured by LSV starting from the E^{ocv} (scan rate, 1 mV s^{-1}, CHI 660C). A platinum wire counter electrode, a saturated calomel electrode (SCE) reference electrode, and bioanode or biocathode working electrode were used to construct a three-electrode electrochemical system.

Supporting Figures

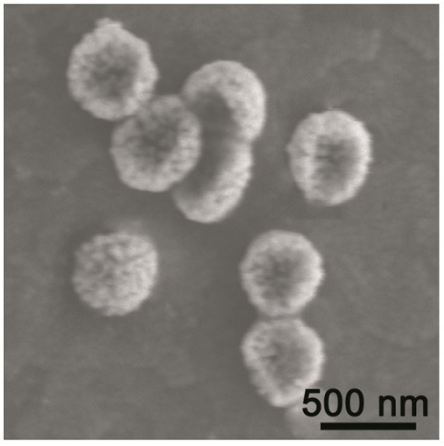

Supplementary Figure 1: SEM image of pAuNB.

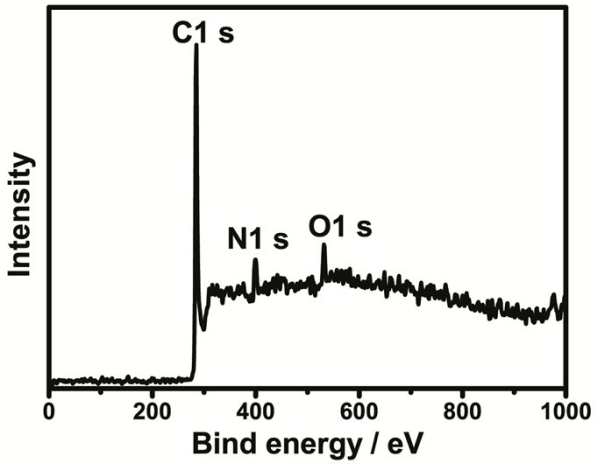

Supplementary Figure 2: XPS of hmNCS. The XPS analysis revealed the weight ratio between C and N is about 10:1.

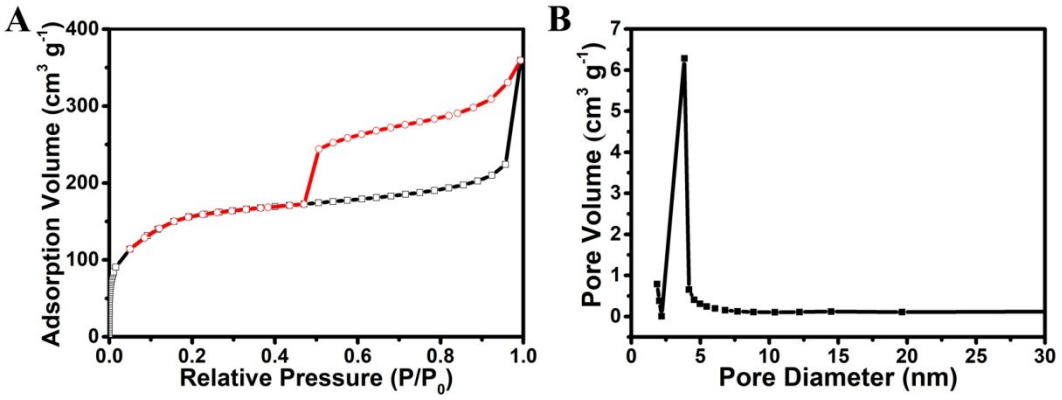

Supplementary Figure 3. Nitrogen adsorption-desorption isotherms (A) and Barrett-Joyner-Halenda (BJH) pore size distributions (B) of $hmSiO_2$.

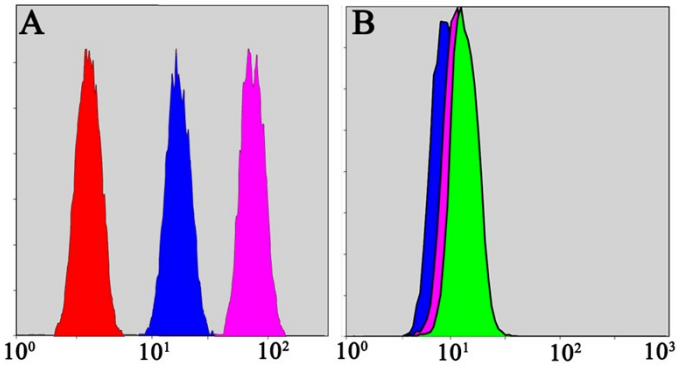

Supplementary Figure 4. Flow cytometry results of K562 cells after incubating with HA@Dox@$hmSiO_2$ (A) and Dox@$hmSiO_2$ (B) nanoparticles for different times. From left to right: 2 h, 4 h and 6 h. With the aid of HA in targeting and preventing the premature release of Dox, the group of HA@Dox@$hmSiO_2$ shows an obviously enhanced uptake into cells over time compared to the group Dox@$hmSiO_2$.

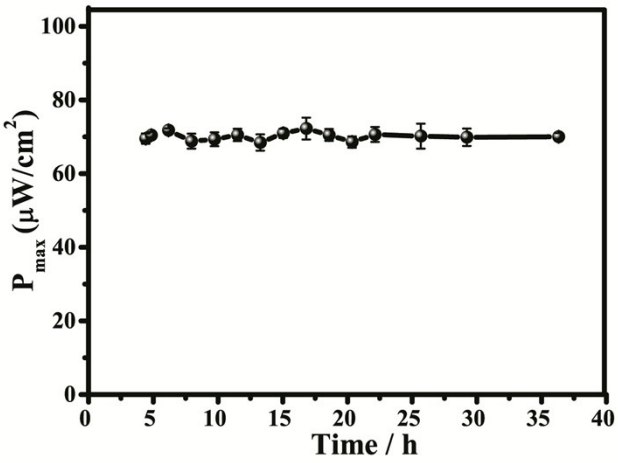

Supplementary Figure 5: Time course of maximum power density generation in DDM-SDSE, where 200 μL RPMI 1640 medium containing 1.0×10^4 K562 cells but without miR-12a was used as electrolyte.

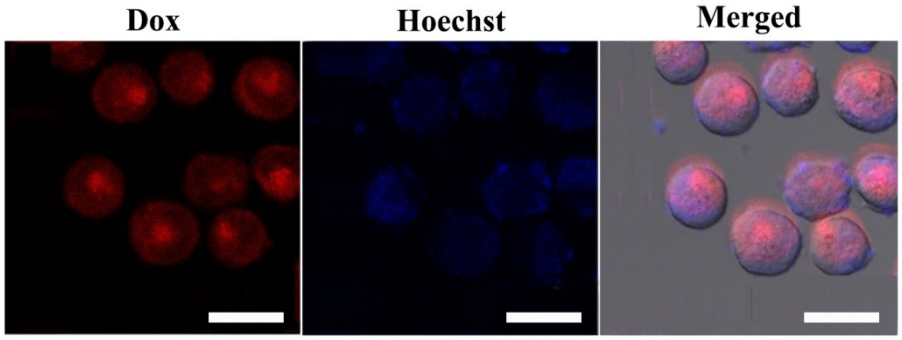

Supplementary Figure 6. CLSM images of K562 cells collected from DDM-SDSE after operation in 1.0×10^4 K562 cells-contained PRMI 1640 medium for 6 h in the presence of 0.1 fM miR-125a. The cells were further stained with Hoechst (blue fluorescence) before imaging, the red fluorescence derived from Dox. Scale bars: 25 μm.

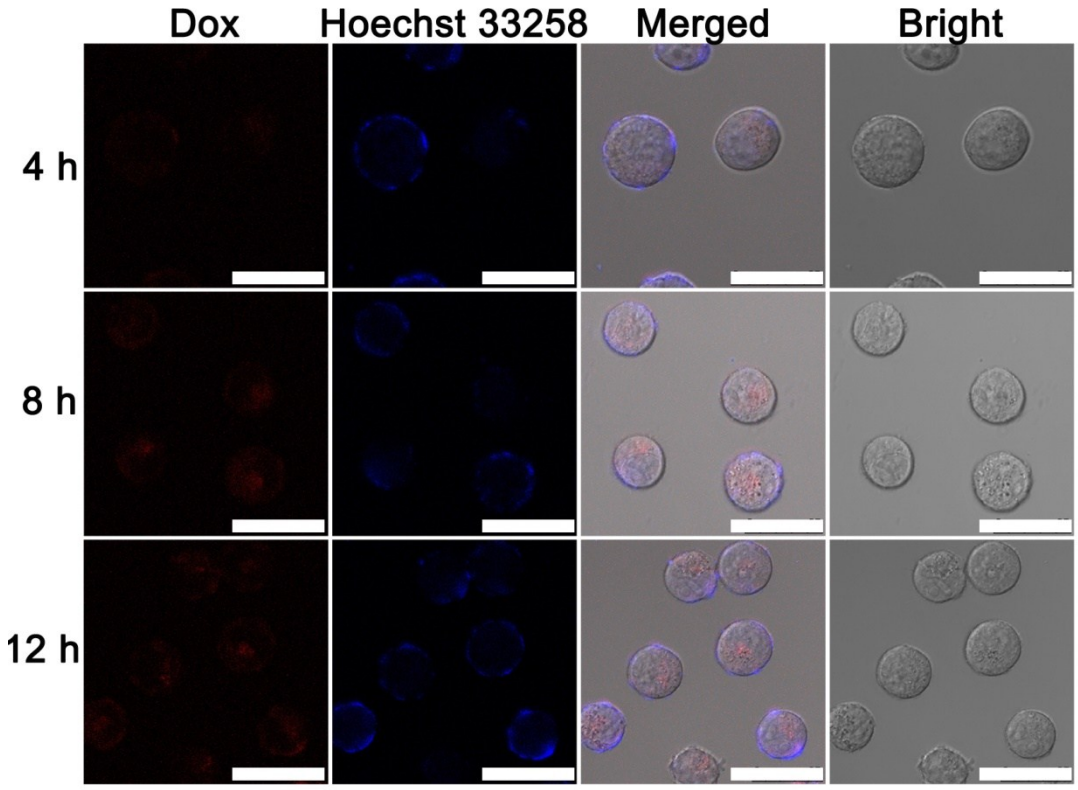

Supplementary Figure 7. CLSM images of K562 cells collected from DDM-SDSE after operation in 1.0×10^4 K562 cells-contained PRMI 1640 medium for different time in the absence of miR-125a. The cells were further stained with Hoechst (blue fluorescence) before imaging, the red fluorescence derived from Dox. Scale bars: 25 μm.

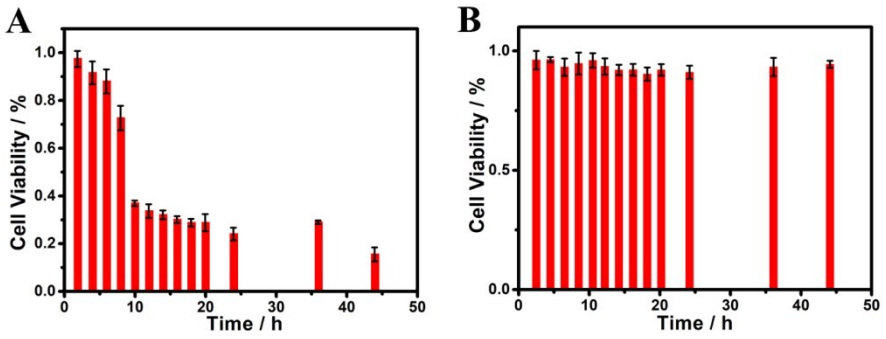

Supplementary Figure 8. The MTT-based viability assay of K562 cells collected from DDM-SDSE after operation in 1.0×10^4 K562 cells-contained PRMI 1640 medium for different time in the presence (A) and absence (B) of 0.1 fM miR-125a. In Figure A, the viability of K562 cells display almost change in first 6 h, indicating that the released drug-loaded during the diagnosis process have not induce the cell apoptosis yet, therefore, the P_{max} have not immediately decreased after the completion of diagnosis. In the following two hours (6 h to 8 h), the viability shows a relative

obvious decrease, suggesting the drug begin to induce the cell apoptosis, and the viability remarkably decreased from 8 h to 10 h, indicating plenty of apoptosis cells appear. As a result, the P_{max} shows a decrease in this period. Finally, the viability keeps no change during 16 h to 36 h, and the number of apoptosis cells no longer increase. Thus, the P_{max} keeps no change after the fully capture of apoptosis cells. In Figure B, almost no change in cell viability was detected during the test time, indicating that the above change in viability is due to the occurrence of various events instead of the possible toxicity from the DDM-SDSE.